The Effect of Hydrogen on the Yield and Flow Stress of an Austenitic Stainless Steel

DANIEL P. ABRAHAM and CARL J. ALTSTETTER

Tensile tests on 310s stainless steel foils, with and without hydrogen, were conducted at temperatures from 77 to 295 K and strain rates from 10^{-3} to 10^{-6}/s. Cathodic charging at elevated temperatures and at very low current densities was used to produce homogeneous solid solutions of hydrogen in this material. The yield stress and flow stress were found to increase with hydrogen content. Discontinuous yielding was observed at room temperature for specimens with hydrogen contents greater than 5 at. pct. The ductility, as measured by the strain to failure, was not critically dependent on hydrogen concentration at 77 and 295 K but was reduced at intermediate temperatures. The changes in mechanical behavior are discussed in terms of hydrogen-dislocation interactions.

I. INTRODUCTION

AUSTENITIC stainless steels are commonly used in hydrogen-rich environments in industry and in space engines where hydrogen is used as a fuel. The diffusivity of hydrogen in these face-centered cubic (fcc) steels is lower and these steels' solubility for hydrogen is higher than in body-centered cubic (bcc) steels; hence, they are thought not to be as susceptible to hydrogen embrittlement as steels with a ferritic or martensitic microstructure. However, in regions of high stresses such as crack tips and notches, there can be a significant accumulation of hydrogen, which could lead to failure. The mechanisms proposed for such hydrogen embrittlement have not been verified. There is controversy between those who believe that the effect of hydrogen is to reduce the cleavage stress and those who believe that its dominant effect is to modify plastic behavior.

The tensile test provides information on macroscopic quantities such as strength, ductility, and work hardening; this information, combined with microscopic observations, can be used to deduce dislocation behavior in the presence of hydrogen. The effect of hydrogen on tensile flow curves has been investigated in several studies, but the results have often been contradictory. The macroscopic experiments of Matsui and co-workers[1,2,3] demonstrated that a decrease in the flow stress occurred in very pure iron in the presence of hydrogen. This effect was ascribed to hydrogen-enhanced dislocation mobility. Kimura and Birnbaum[4] demonstrated similar effects in nickel. Bernstein[5] suggested that hydrogen reduced the lattice friction stress, meaning that a hydrogen-associated dislocation could move more easily in a lattice than a dislocation either without hydrogen or with a carbon or nitrogen atmosphere. Lunarska[6] reviewed the effects of hydrogen on the plasticity of iron and noted that the predominant effect of hydrogen appeared to be the increase in screw dislocation mobility, probably due to a reduction in dislocation line tension. Sirois and Birnbaum determined that hydrogen decreased the activation energy for plastic deformation in nickel.[7] Robertson and co-workers concluded from transmission electron microscopy (TEM) observations that hydrogen from a gaseous environment can increase the ease of nucleation and motion of dislocations in nickel, stainless steel, and other metals.[8–11]

In contrast to the observations of enhanced dislocation nucleation and increased dislocation velocities in the presence of hydrogen are the reports of solute hydrogen strengthening in metals. Boniszewski and Smith[12] observed hydrogen hardening in pure nickel and reported serrated yielding in the presence of hydrogen. Watson *et al.*[13] studied the effects of cathodically charged hydrogen in pure aluminum and found that hydrogen increased the yield and tensile strengths while reducing the ductility of the metal. West and Louthan[14] reported that hydrogen raised the yield stress and reduced the interfacial strength of 21-6-9 fcc stainless steel. The studies on 304L stainless steel by Caskey[15] and Holbrook and West[16] showed that hydrogen caused an increase in the yield stress of the metal. Asano and Otsuka[17,18] observed increases in flow stress due to hydrogen in iron and mild steel. Other instances of hydrogen-induced strengthening in iron[19] and stainless steels[20,21] have also been reported. The increases in yield strength in the presence of hydrogen have been attributed to hydrogen-dislocation interactions, where the effect of hydrogen is the inhibition of dislocation motion and/or reduced dislocation cross slip.

The experimental procedures used to demonstrate hydrogen-induced hardening have often been subject to severe criticism. The presence of hydrogen concentration gradients leading to dislocation injection, surface hardening/softening, the possibility of phase transformations, and the formation of stress-induced hydride at dislocation cores have been invoked to explain the strengthening effects and serrated yielding observed in hydrogenated materials. Myers *et al.*[22] have suggested that the intrinsic softening effect of hydrogen can be observed only if the aforementioned experimental artifacts are avoided, but the hydrogen-induced hardening in pure iron at temperatures less than 200 K[1,2,3] is generally considered to be a real effect of hydrogen. Hirth[23] has suggested that the nucleation of double kinks on edge dislocations is made difficult by hydrogen below 200 K, and this inhibiting effect of hydrogen on dislocation

DANIEL P. ABRAHAM, formerly Graduate Student, Department of Materials Science and Engineering, University of Illinois at Urbana–Champaign, is Postdoctoral Associate, Chemical Technology Division, Argonne National Laboratories, Argonne, IL 60439. CARL J. ALTSTETTER, Professor, is with the Department of Materials Science and Engineering, University of Illinois at Urbana–Champaign, Urbana, IL 61801.

Manuscript submitted February 28, 1994.

Table I. Chemical Composition of 310s Stainless Steel (Weight Percent)

	C	Mn	P	S	Si	Cr	Ni	Mo	Cu	Fe
310s	0.018	1.77	0.022	0.001	0.67	25.37	19.37	0.4	0.17	bal

motion causes the observed hardening. The intrinsic effect of hydrogen, whether hardening or softening, is still a subject of much controversy and undoubtedly depends on the material under consideration.

The effect of hydrogen on austenitic stainless steels has been studied by numerous investigators.[24–33] The degree of embrittlement in hydrogen is said to be inversely proportional to the stacking fault energy of these steels.[34] Austenitic stainless steels such as 310s (a low carbon variant of 310), that have a relatively high stacking fault energy (greater than 35 mJ/m^2), were initially claimed to be immune to hydrogen effects until Whiteman and Troiano[26] demonstrated that embrittlement of 310 occurred at high hydrogen contents. The planar slip tendency of austenitic stainless steels probably makes them more susceptible to hydrogen effects, with the steels exhibiting the greatest slip planarity, for whatever reason, being the most affected.

The internal friction experiments by Peterson *et al.*[33] on 310 stainless steel suggested that hydrogen-dislocation interactions could play a significant role in the deformation behavior of this metal. Later experiments by Louthan *et al.*[29] on 310 and other austenitic stainless steels confirmed this observation. Burke *et al.*[20] performed a series of experiments in which internal hydrogen was shown to increase the flow stress and substantially decrease the ductility of various austenitic stainless steels. Their experiments demonstrated significant hydrogen-dislocation interactions. Ulmer and Altstetter showed significant hardening of stainless steel by hydrogen and discontinuous yielding at approximately 5 at. pct hydrogen.[21]

The bulk solubility of hydrogen in 310s steel, in equilibrium with one atmosphere of hydrogen gas at 298 K, is only about 0.01 at. pct.[35] Hydrogen concentrations far greater than this equilibrium solubility will be considered in this study in order to accentuate the effects of hydrogen and to simulate the material condition at dislocations or at the tip of a propagating crack, where stress-enhanced hydrogen concentrations are expected. The stress-strain relations for homogeneous 310s-hydrogen alloys will be observed for a range of temperatures and strain rates, with the objective of quantifying the crucial role of hydrogen in behavior modification. Additional mechanical behavior determinations and microscopic observations are described in the second article.[36]

II. EXPERIMENTAL PROCEDURE

Sheets of 50-μm-thick cold-rolled 310s steel, having the chemical composition listed in Table I, were cut along the direction of rolling into rectangular pieces, 125-mm long and 50-mm wide. They were annealed at 1100 °C for 15 minutes under a vacuum of approximately 10^{-4} Pa and then quenched in water. The resulting grain size was between 10 and 15 μm. In order to produce a homogeneous distribution of hydrogen in austenitic stainless steel within a reasonable period of time near room temperature, the sheets were first electrochemically thinned. The annealed sheets were cut into 50-mm squares, and a constant voltage of about 8 V was maintained in a 4:1 perchloric acid-glacial acetic acid mixture at 0 °C. The piece was placed between two larger cathodes of 310s stainless steel. The current density decreased as a polishing film formed over the specimen surface and then reached a constant value of about 20 mA/cm^2. The anode was removed from the solution every 5 minutes, cleaned in distilled water, thoroughly dried, and then reintroduced into the solution. This procedure was necessary to prevent grooving and nonuniform thinning of the specimen. The process was repeated until the thickness was 30 μm. The electropolishing rate was calculated to be about 0.6 μm/min. After electropolishing, the stainless steel foils appeared shiny to the naked eye and smooth under the optical microscope.

Hydrogen was introduced into the foils by cathodic charging at slightly elevated temperatures. Each foil, supported by a mylar frame, formed the cathode in a 0.5M H_2SO_4 + 0.1 g/L $NaAsO_2$ solution, while two 50 × 50 mm platinum foils placed on either side of the foil formed the anode. Nitrogen gas was continuously bubbled through the solution from a porous PYREX* frit to keep the solution constantly stirred, to reduce the amount of oxygen in solution, and to prevent bubbles of hydrogen from forming on the specimen and hence causing nonuniform charging.[37,38] All glassware and electrodes were cleaned following the recommendations of Coyle *et al.*[39] Previous work[40] on the cathodic charging of hydrogen into 310s stainless steels had established that at charging temperatures between 35 °C and 75 °C, only the fcc austenite phase was stable until the hydrogen content exceeded 16 at. pct, at which point a hydrogen-rich fcc phase, γ^*, and a hydrogen-rich hexagonal phase, ε^*, formed in the specimens at low temperatures (35 °C). Since the hydrogen contents used in this study did not exceed 10 at. pct and the solution temperature for charging was chosen to be 80 °C, it may be assumed that no second phases were produced by hydrogen charging and subsequent cooling to room temperature. The charging time of 12 hours was roughly twice that necessary for diffusion-controlled saturation at the foil center.[41] The amount of hydrogen was controlled by changing the applied current density, which never exceeded 0.5 mA/cm^2. Even these small current densities were capable of introducing high concentrations of hydrogen into the material. The specimen surface remained shiny after hydrogen charging. The foils were removed from the charging solution, rinsed with distilled water, and stored in liquid nitrogen to prevent hydrogen loss. The hydrogen content of each foil was measured volumetrically after outgassing at high temperatures. Titanium-hydrogen standards, obtained from the National Bureau of Standards (Gaithersburg, MD) NBS, were used to verify the measurement procedure. Several measurements were made on specimens cut from the charged foil and average values were calculated. Some of these measurements were made before and after the tensile test

*PYREX is a trademark of Corning Glass Works, Corning, NY.

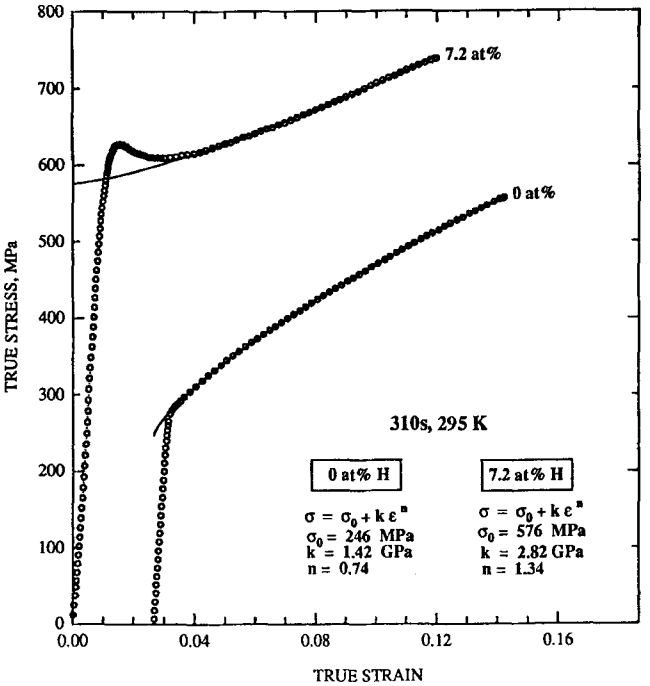

Fig. 1—Stress-strain curve fits using Eq. [1] (solid line) for a hydrogen-free specimen and for a specimen containing 7.2 at. pct hydrogen strained at 5.5×10^{-5}/s. The curves are offset for clarity. Only every fifth data point (open circles) is shown in the plastic regime. The fitting parameters are cited in the figure.

and some were made on specimens exposed to air for the period of a tensile test, which usually lasted about 40 minutes. The relative variation in calculated values was within ±10 pct. There was no significant difference between tested and untested specimens cut from the same 50-mm square sheet.

Tensile specimens, 5-mm wide by 30-mm long, were cut from the hydrogen-charged foils along the direction of rolling; the edges of the foils were discarded because of the higher local current density.[42] Specially designed stainless steel grips were used to test the thin foil specimens so that mounting-induced deformation was minimized; the gage length was taken as the distance between the grips. Stress-strain curves of hydrogen-free and hydrogenated specimens were obtained at various constant (±3 pct) extension rates, and the output voltage of the load cell was recorded by a data acquisition system. To eliminate variability due to specimen dimensions, all stress-strain curves at the same temperature and strain rate were normalized to the same modulus. This gave negligible errors in the plastic portion of the curve. Room-temperature testing was in air, while testing at subambient temperatures was in various liquid media.

III. RESULTS

Before the foil was subjected to cathodic charging, a representative sample was cut from every annealed batch and tensile tested at room temperature to characterize the variability in stress-strain curves of the hydrogen-free material. The yield stress variation calculated at 0.1 pct plastic strain was 270 ± 15 MPa. The plastic regime of the true stress-strain curves was fit to Ludwik's equation:[43]

$$\sigma = \sigma_0 + k\varepsilon^n \quad [1]$$

where σ is the true stress, ε is the true strain, n is the strain-hardening exponent, and k and σ_0 are fitting parameters. This equation provided an excellent fit for specimens tested at various temperatures, hydrogen contents, and strain rates, except in the vicinity of discontinuous yielding. Figure 1 compares measured data with Ludwik's equation for stress-strain curves of a hydrogen-free specimen and for a specimen containing 7.2 at. pct hydrogen. The work-hardening rate as a function of strain was obtained by differentiating Eq. [1] with respect to the true strain. The average value of the strain-hardening exponent for a hydrogen-free specimen was calculated to be 0.72 ± 0.03, while the average work-hardening rate was 2.16 GPa per unit value of the true strain. For specimens that showed a yield point discontinuity, the work-hardening rate was plotted only after the lower yield stress.

The foils were mechanically tested at temperatures ranging from 295 to 77 K at strain rates that varied from 1.4×10^{-3} to 1.1×10^{-6}/s. Some of the specimens were degassed at room temperature for periods of over a week and then mechanically tested. The yield stress of the degassed specimens was about the same as for uncharged specimens, and their fracture surfaces resembled those of uncharged specimens. It was hence concluded that hydrogen charging was a reversible process and that no significant damage occurred during the introduction and subsequent removal of hydrogen from the specimens.

The highlights of the various experiments will now be presented. First, the effect of hydrogen on the behavior of 310s specimens tested at 295 K will be shown, followed by the stress-strain plots at 77 K. The effects of strain rate and temperature on 310s specimens at various hydrogen contents will then be presented.

A. *Testing Temperature: 295 K*

At concentrations less than 0.18 at. pct, hydrogen did not have a statistically significant effect on the 310s specimens, since all the tensile curves were observed to lie within the band of uncertainty of the hydrogen-free material, shown by the cross-hatched band in Figure 2. However, at 0.25 at. pct hydrogen (Figure 2), strengthening was apparent: both the yield and flow stress were increased. Figure 3 shows the effect of hydrogen at higher concentrations. As the hydrogen content was increased, both the yield and flow stresses increased. Above 5 at. pct hydrogen, there was a yield point discontinuity; that is, an upper and lower yield point were visible in the tensile curves. Above this concentration, the upper yield stress increased and the lower yield stress decreased with hydrogen content (inset of Figure 3). It is interesting to note that the increase in flow stress parallels the increase in the yield stress until about 5 at. pct hydrogen; that is, the entire stress-strain curve is raised by adding hydrogen to this alloy. Above 5 at. pct, the flow stress actually decreased with hydrogen content. The macroscopic strain to failure was not greatly affected by hydrogen except at very high contents (9.2 at. pct in Figure 3). At even greater concentrations of hydrogen, the stainless steel specimens were very brittle and could easily be crumpled to pieces by hand. The effect of hydrogen on the work-hardening rate is shown in Figure 4, where Eq. [1] suggests

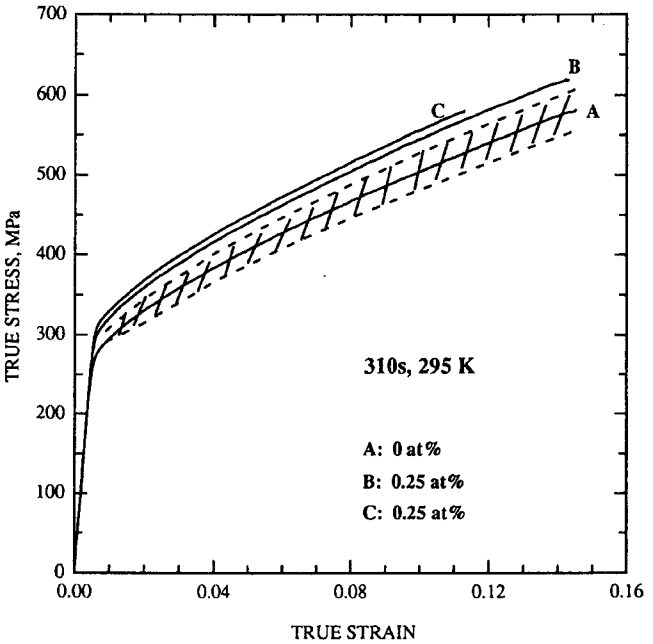

Fig. 2—Effect of 0.25 at. pct hydrogen on the mechanical behavior of 310s at 295 K and at a strain rate of 5.5×10^{-5}/s. The scatter in the data for several hydrogen-free specimens is shown by the cross-hatched band.

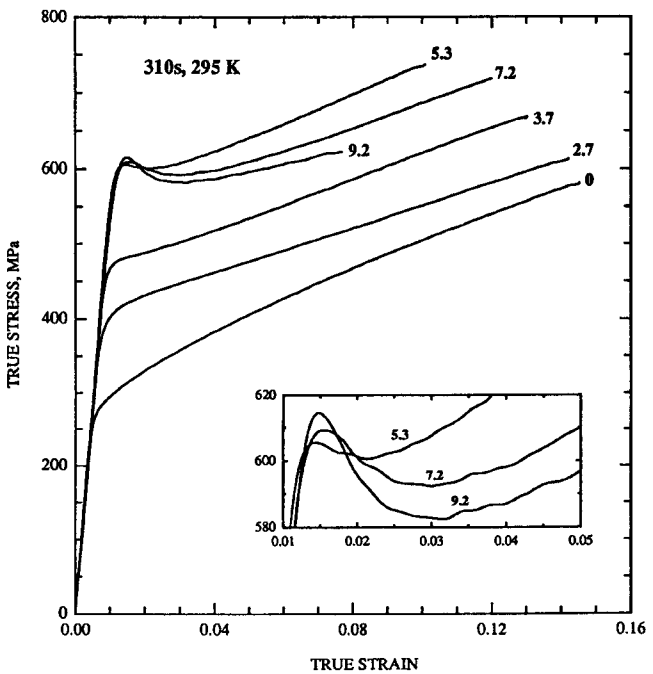

Fig. 3—Stress-strain curves at various hydrogen contents (atomic percent) at 295 K and at a strain rate of 5.5×10^{-5}/s. The inset is a magnified view of the yield discontinuity.

a linear log-log plot with a slope of $(n - 1)$. Table II lists the various parameters used in calculating the work-hardening rates shown in Figure 4. It is apparent that the work-hardening rate at small strains decreases with an increase in hydrogen content, while at high strains, the rate appears independent of the concentration of hydrogen. The hydrogenated 310s specimens behaved similarly when tested at strain rates both greater and less than 5.5×10^{-5}/s. In general, the yield and flow stress increased and the work-hardening rate decreased with hydrogen content.

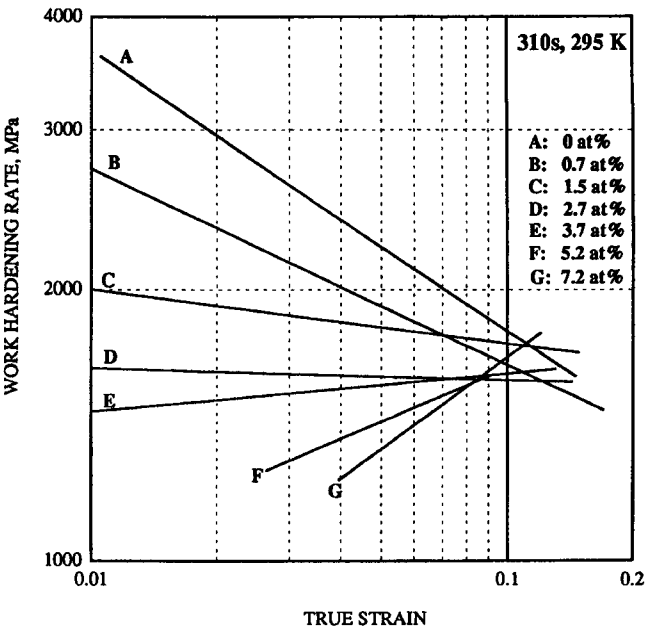

Fig. 4—Work-hardening rate *vs* true strain for various hydrogen concentrations at 295 K and at a strain rate of 5.5×10^{-5}/s.

Table II. Parameters Used to Fit the Flow Curves in Figure 3 and to Calculate the Work-Hardening Rates in Figure 4 (T = 295 K)

Curve	H Content (At. Pct)	σ_0 (MPa)	k (MPa)	n
A	0	251	1314	0.69
B	0.7	289	1312	0.78
C	1.5	408	1658	0.94
D	2.7	412	1601	0.99
E	3.7	469	1749	1.04
F	5.2	495	2209	1.19
G	7.2	576	2818	1.34

B. *Testing Temperature: 77 K*

Figures 5 and 6 show the stress-strain curves and work-hardening rates for specimens tested at 77 K at a strain rate of 5.5×10^{-5}/s for hydrogen contents from 0 to 7.1 at. pct. Just as at 295 K, the yield and flow stress increased with hydrogen content at all strain rates studied. However, there were definite differences between 295 and 77 K behavior. The yield and flow stresses at 77 K were about double those at 295 K. The work-hardening rates were higher and increased with hydrogen content (Figure 6 and Table III) in contrast to the results at 295 K, where the work-hardening rate decreased with increasing concentrations of hydrogen (Figure 4). The yield point discontinuity, when observed, was not as prominent as it was for room-temperature testing. There was no definite trend in the strain to failure values, though they were still mostly in excess of 0.1, even at hydrogen contents greater than 5 at. pct.

C. *Effect of Strain Rate and Temperature*

The effect of strain rate at a hydrogen content of 5.3 at. pct at two different temperatures (295 and 77 K) is shown in Figure 7. It may be noted that both the yield and flow

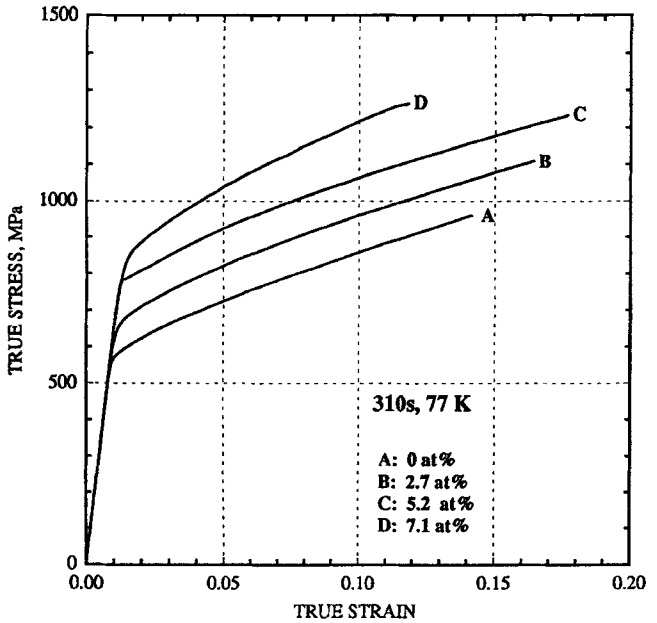

Fig. 5—Stress-strain curves for various hydrogen concentrations at 77 K and at a strain rate of 5.5×10^{-5}/s.

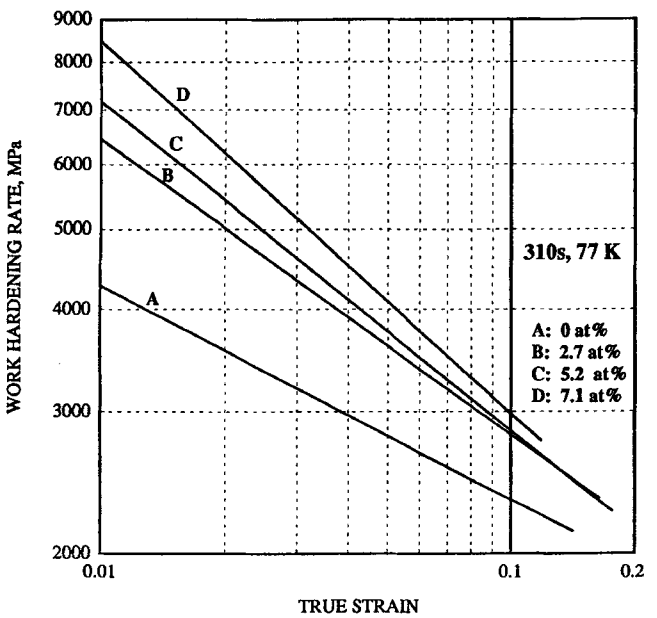

Fig. 6—Work-hardening rate curves at a strain rate of 5.5×10^{-5}/s for various concentrations of hydrogen concentrations at 77 K.

Table III. Parameters Used to Fit the Flow Curves in Figure 5 and to Calculate the Work-Hardening Rates in Figure 6 (T = 77 K)

Curve	H Content (At. Pct)	σ_0 (MPa)	k (MPa)	n
A	0	534	1812	0.74
B	2.7	586	1891	0.64
C	5.2	670	1832	0.60
D	7.1	637	1955	0.54

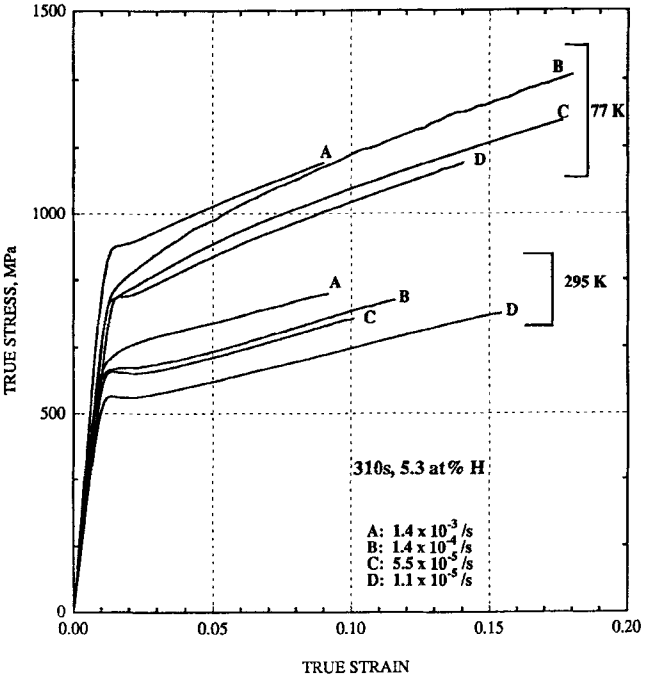

Fig. 7—Stress-strain curves for various rates of strain at a hydrogen content of 5.3 at. pct at 295 and 77 K.

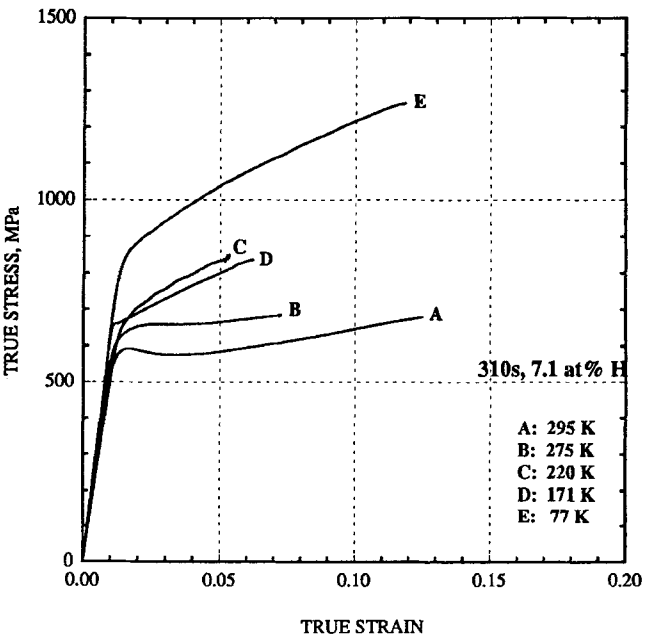

Fig. 8—Stress-strain curves at various temperatures for a hydrogen content of 7.1 at. pct and at a strain rate of 5.5×10^{-5}/s.

stress increased as the strain rate increased. The yield point discontinuity progressively disappeared as the strain rate was increased at 295 K and was absent at 1.4×10^{-3}/s. Smaller yield drops were seen at 77 K and only at strain rates of 1.4×10^{-3} and 1.1×10^{-5}/s. The effect of temperature at 7.1 at. pct hydrogen and a strain rate of 5.5×10^{-5}/s is summarized in Figure 8. The yield and flow stress increased with a decrease in temperature. A minimum in the value of the macroscopic ductility occurs at 220 K. It is interesting to note that for specimens with a hydrogen content of 7.1 at. pct, the largest failure strains are obtained at the extreme temperatures, and at 171 to 275 K, the elon-

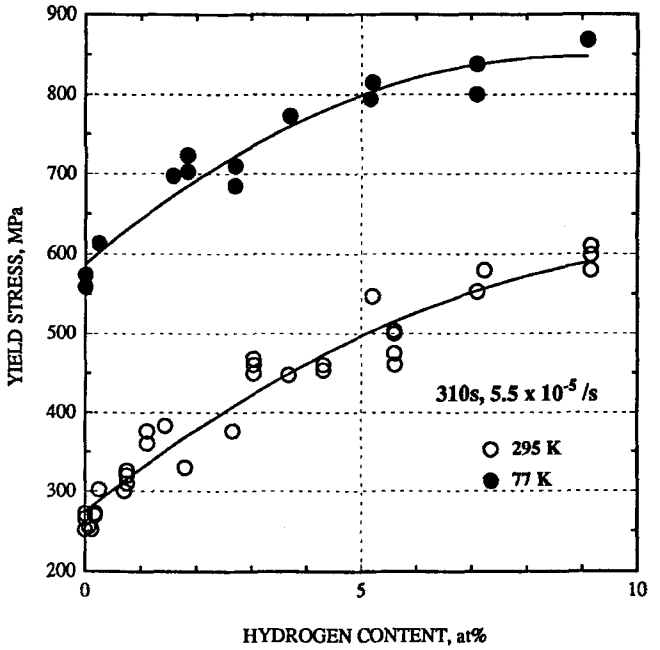

Fig. 9—Yield stress *vs* hydrogen content at 295 and 77 K at a strain rate of 5.5×10^{-5}/s.

Table IV. Interstitial Solute Hardening at Room Temperature (Shear Modulus, $G \approx 80$ GPa[44] for Listed Metals)

Metal	Solute	Typical Hardening per At. Pct of Solute
Bcc iron	carbon	$G/20$[45]
Nickel	carbon	$G/1000$[45]
15 Ni-15 Cr stainless steel (fcc)	carbon	$G/1200$[46]
Austenitis stainless steel	nitrogen	$G/800$[46,47]
310s stainless steel	hydrogen	$G/2000$ (this work)

gation is reduced to about half of that at lower or higher temperatures for this combination of strain rate and hydrogen concentration. Figure 9 is a plot of yield stress *vs* hydrogen content at a strain rate of 5.5×10^{-5}/s for the extreme values of the temperatures tested; that is, 295 and 77 K. It may be noted that the increase is not linear but rather the relative increase per atomic percent decreases at the higher hydrogen contents.

IV. DISCUSSION

A. *Strengthening by Hydrogen*

The introduction of hydrogen into 310s stainless steel resulted in strengthening; both the yield and flow stress were increased in the temperature range from 77 to 295 K and for macroscopic strain rates from 1.4×10^{-3} to 1.1×10^{-6}/s. This implies that the dislocation sources and the movement of dislocations are inhibited by hydrogen in some manner. Solid solution strengthening can result from a random, ordered, or segregated distribution of atoms. If the hydrogen atoms order themselves around the matrix atoms in such a way as to form a second phase, either precipitation or dispersion hardening could occur, depending on the size, misfit, and distribution of the precipitates. Table IV compares the hardening effects of interstitial solutes in fcc and bcc metals. It is obvious that although the hardening due to hydrogen is two orders of magnitude smaller than that of carbon in bcc iron, it is only about a factor of 2 smaller than the effects of carbon and nitrogen in fcc nickel and stainless steel. This result is especially significant because hydrogen is a much smaller atom than either carbon or nitrogen. Ledbetter and Austin[48] rationalized dilatation due to interstitial carbon and nitrogen in 304 stainless steel using a simple rigid sphere model. Hydrogen, like carbon and nitrogen, resides in the interstitial octahedral site of the austenite lattice.[49,50,51] Assuming a lattice of equal sized rigid spheres, the radius of the largest sphere that can fit into the octahedral site of austenite is 52 pm. The covalent radii of the carbon and nitrogen atoms are 89 and 85 pm, respectively. Since their size exceeds that of the octahedral site, these atoms are expected to distort the fcc lattice.[48] Using the covalent radius of hydrogen, 37 pm,[52] it could occupy an octahedral site without causing any elastic distortion. The rigid sphere model would require a hydrogen atom of 65 pm to account for Ulmer and Altstetter's value of $\Delta a/a_0 \approx 7.1 \times 10^{-4}$, where Δa is the change in the lattice parameter per atomic percent hydrogen and a_0 is the lattice parameter.[40] This leads to the following possibilities: (a) the rigid sphere model is overly simplified and electronic effects must be taken into account; and (b) more than one hydrogen atom may be associated with an octahedral site, that is, clusters of hydrogen atoms may be present at some of the octahedral sites. Internal friction studies of hydrogen in deformed nickel[53] suggest dislocation interactions with pairs of hydrogen atoms which may be present in adjacent octahedral sites. Even if the static strain field of individual hydrogen atoms is insignificant compared to other dislocation obstacles in the metal, clusters or atmospheres of hydrogen may be involved in the strengthening of the austenite lattice.[7]

1. *Hydrogen Atmospheres*

Ulmer and Altstetter[21] have proposed that discontinuous yielding behavior is a consequence of hydrogen atmosphere locking of Frank–Read and other dislocation sources. Once the first dislocation in a source breaks free from its atmosphere and multiplies, the stress required to continue operating that source would be lower than the stress required to unlock another source. A limited number of dislocation sources will operate, each producing a cascade of dislocations, thus localizing strain on fewer planes. The increase in flow stress would be a combination of two effects: (1) drag by hydrogen atmospheres on slowly moving dislocations and (2) solid solution hardening by hydrogen atoms distributed throughout the lattice.

The elastic interaction of a solute atom with an edge dislocation has the following angular and radial distribution:[54]

$$E_B = \frac{Z \sin \theta}{r} \qquad [2]$$

where

$$Z = \frac{\mathbf{b}\,(1 + \nu)\,G\delta\nu}{3\pi\,(1 - \nu)} \qquad [3]$$

The term E_B is the binding energy of the hydrogen atom to

the dislocation, **b** is the magnitude of the Burgers vector, G is the shear modulus, ν is Poisson's ratio, r is the distance from the core, and δv is the volume change of the lattice upon the introduction of one hydrogen atom. For hydrogen in 310s steel, $\delta v/\Omega = 0.2$,[40] where Ω is the mean atomic volume of the solvent atom. For 310s stainless steel, $\delta v = 1.71 \times 10^{-30}$ m^3, $\nu = 0.3$, $\mathbf{b} = 2.5 \times 10^{-10}$ m, and $G = 80$ GPa. Thus,

$$E_B = 6.8 \times 10^{-30} \frac{\sin \theta}{r} \quad [4]$$

The binding energy will be maximum when $\sin \theta = -1$ and r is the core radius. Letting $r = \mathbf{b}$,[54] we obtain the maximum value

$$(E_B)_{\max} = -2.7 \times 10^{-20} \text{ J} = -0.17 \text{ eV}$$

This value of the maximum binding energy between a hydrogen atom and an edge dislocation in austenitic stainless steels is comparable to the values mentioned in the literature.[33,55,56]

If sufficient time is available for diffusion, hydrogen atoms will form atmospheres around dislocations.[57] Cottrell and Bilby[58] used the Boltzmann approximation,

$$C = C_0 \exp(-E_B/kT) \quad [5]$$

where C and C_0 are the atom fractions of the solute in the defect field and remote from the defect, respectively, to estimate the adsorption of solute in the stress field of dislocations. Beshers[59] noted the inadequacy of the Boltzmann approximation and suggested the use of the Fermi–Dirac form:

$$\frac{C}{1-C} = \frac{C_0}{1-C_0} \exp \frac{-E_B}{kT} \quad [6]$$

The atmospheres may be considered dense for $C \geq 0.5$.[60] Letting $E_B = (E_B)_{\max} = -0.17$ eV, for $T = 295$ K and $C = 0.5$, $C_0 = 0.0012$. Very small bulk concentrations of hydrogen are hence required to create a dense atmosphere around edge dislocations using $r = \mathbf{b}$ for the core radius. If $r = 4\mathbf{b}$, $(E_B)_{\max} = -0.04$ eV, and for $T = 295$ K and $C = 0.5$, a bulk concentration of $C_0 = 0.17$ is required to produce a dense atmosphere, far higher than those used in this work. These calculations assume that $E_B \neq f(C)$, an assumption that has been challenged recently.[61]

Dislocation locking or drag by hydrogen atmospheres must be reconciled with *in situ* TEM observations by Birnbaum *et al.*, who showed that hydrogen increased the mobility of screw, edge, and mixed dislocations in nickel and stainless steels as well as other metals.[8–11] This has been attributed to screening of the dislocation stress field by its hydrogen atmosphere, thus making it interact less strongly with short-range obstacles.[61] If a hydrogen atmosphere enhances dislocation motion, then the increases in yield and flow stress of 310s steel in hydrogen might be due to the formation of a precipitate that locks dislocations. This may be analogous to the effect of carbon in mild steel, where either dislocations can act as precipitate nuclei on which carbon atoms may form particles of carbide (quench aging) and/or carbon can form atmospheres around dislocations (strain aging).[62] There is competition between the two aging processes. Similarly, in 310s stainless steel, there could be competition between the formation of a hydrogen atmosphere around a dislocation which may enhance its mobility and the formation of a hydride at the core.

2. *Dislocation Locking by Hydrides*

In 310s steel, a hydrogen-rich phase, γ^*, is known to form under conditions of strong cathodic charging.[40,63] Ulmer and Altstetter[40] found that in 310s stainless steel, homogeneously charged and cooled to 193 K, γ^* was not detectable by X-ray diffraction at lattice concentrations less than 16 at. pct hydrogen. Their X-ray measurements indicated that the γ^* phase occupied a volume 6 pct greater than the hydrogen-saturated austenite matrix. When the hydrogen content was increased beyond the concentration at which γ^* was observed, the intensity of the γ^* peak increased at the expense of the austenite, γ, matrix peak. Furthermore, the γ^* was unstable and reverted to γ on outgassing. They concluded that the hydrogen-310s stainless steel phase diagram probably included a miscibility gap. By a very long extrapolation of their limited data to 77 K, it is estimated that austenite would be saturated at hydrogen concentrations above 0.2 at. pct, while at 295 K, the bulk hydrogen concentration needs to be approximately 15 at. pct.

Thus, the γ^* phase would not form at 295 K at any of the concentrations in our experiments. However, the volume increase due to γ^* formation would indicate that this phase can be induced at lower hydrogen concentrations by tensile stresses. The hydrogen concentration at which γ^* would form under the influence of uniaxial tensile stress can be estimated by[64]

$$C_s = C_0 \exp -(\sigma_s \Delta V_{\gamma-\gamma^*}/RT_\sigma) \quad [7]$$

where C_s and C_0 are the solvus compositions under stress and in the stress-free solution, respectively, T_σ is the solvus temperature under stress, σ_s is the hydrostatic component of the stress and can be assumed to be a third of the uniaxial applied stress σ_A, and $\Delta V_{\gamma-\gamma^*}$ is the molar volume change on formation of the γ^* phase from the γ solid solution. The value of $\Delta V_{\gamma-\gamma^*}$ can be estimated by assuming that the volume change due to hydrogen in solution is the same for γ and γ^*. At 295 K, a hydrogen-free specimen yields at around 270 MPa, thus σ_s would be about 90 MPa at yield. At this value of the applied stress, the hydrogen concentration required to form the γ^* phase would be decreased only from 14.6 at. pct to approximately 14 at. pct.

The preceding arguments show that γ^* formation in the bulk phase is not expected at 295 K. However, at localized regions, such as dislocation cores, nucleation of γ^* might be possible, even at very low bulk hydrogen concentrations. If nucleated at dislocation cores, γ^* may be effective in locking dislocations and dislocation sources. Hirth and Carnahan[65] proposed that the core region of a dislocation in bcc iron could accommodate many hydrogen atoms per plane cut by the dislocation. They concluded that site saturation to some extent is tantamount to hydride formation in a cylindrical surface surrounding the core. Kirchheim *et al.*[66,67] noted a zone of extended hydrogen segregation at dislocations in Pd. Kimura and Birnbaum[68] attributed the increase in flow stress observed during cathodic charging of nickel to hydride formation at dislocation cores. New phases have been detected at dislocation cores in other systems, for example, nitrides in iron[69] and oxides in silicon.[70] The main drawback of the hydride locking theory

is that hydrides at dislocation cores have not been observed in any material. Additionally, though the hydride theory might explain the observed increases in yield stress, it is not able to explain the increased flow stresses with hydrogen content, because once the stabilizing dislocations have been pulled away, their hydride rapidly dissolves. Besides, a hydride that is only 1**b** to 5**b** in diameter would be easily cut.

B. *Yield Point Discontinuity*

The explanation of discontinuous yielding proposed by Cottrell[57] was later extended by Johnston and Gilman[71] and by Hahn.[72] Their model suggests that the discontinuous yield point is a consequence of at least four factors: (1) low velocities and/or a small number of mobile dislocations initially, (2) rapid multiplication of mobile dislocations, (3) stress dependence of dislocation velocity, and (4) rapid increase in the average distance that dislocations move. It is commonly accepted that the classic case of discontinuous yielding in mild steel (bcc) is due to the locking of dislocations by carbon and nitrogen atoms. Rogers studied the role of hydrogen in discontinuous yielding of Armco iron and mild steel.[73,74,75] The yield point normally present at room temperature was suppressed by hydrogen.[74,75] However, when Rogers prestrained specimens to free the dislocations from carbon and nitrogen and then introduced hydrogen by cathodic charging, he found that a yield point appeared if the specimens were subsequently tested below 190 K. The magnitude of the load drop increased with decreasing test temperature. He suggested that suppression of the yield point at room temperature was due to hydrogen atmospheres around dislocation loops after they broke free from carbon and nitrogen, thereby lowering the energy of the freed loop and reducing the activation energy required to free a loop. At low temperatures, the hydrogen atmosphere was no longer mobile, and it caused pinning. De Kazinczy argued that hydrogen suppresses the yield point by producing centers of internal stress and not by facilitating the unlocking of dislocation.[76] Hydrogen is known to produce rounded yield points in molybdenum, and the effect has been attributed to a reduction in dislocation mobility.[77]

Discontinuous yielding is not commonly observed in fcc nickel and austenitic stainless steels, despite the relatively large amount of interstitial solute that can be dissolved. This is presumably due to the isotropic distortion of the lattice by interstitial atoms that results in a relatively small dislocation-interstitial solute interaction energy and only a second-order interaction between interstitial solute and screw dislocations. Guntner and Reed observed rounded yield drops in hydrogen-free 304 but not in 310 stainless steel deformed at 77 K.[78] In our experiments and those of Ulmer and Altstetter,[21] yielding at room temperature was smooth and continuous in hydrogen-free 310 alloy but became progressively less so as the hydrogen content was increased. At 5 at. pct hydrogen and above, yield drops were observed (Figure 3). It could be argued that like carbon in bcc iron, dense hydrogen atmospheres can lock dislocations at high enough solute contents, because at room temperature, hydrogen mobility is so much lower in the fcc than in the bcc phase. The yield point discontinuity is produced when the dislocations are freed from their atmospheres and/or can multiply sufficiently rapidly. However, at 77 K, the driving force to form dense atmospheres is greater, and therefore, pronounced yield drops would be expected but were not observed in our experiments. Perhaps, the mobility of dislocations is too low even without atmospheres. Alternatively, at the high stresses involved, other dislocation sources can be progressively, not abruptly, activated. The minute yield points seen at 77 K were quite similar to those observed by Boniszewski and Smith[12] in hydrogen-charged nickel deformed at temperatures below 120 K. We carried out a few strain aging tests in which high hydrogen content specimens were strained through the Luders band region and then aged.[36] No yield drop was observed upon reloading; yielding was smooth and the flow curve was a continuation of that before aging. Clearly, there are anomalies in the discontinuous yielding behavior that require further experiments and perhaps a reassessment of the theory.

Birnbaum and co-workers have proposed that hydrogen-enhanced localized plasticity (HELP) observed in environmental cell TEM experiments[8–11] and in macroscopic experiments on nickel[79] is a result of hydrogen atmospheres that can shield the stress field of a dislocation. The moving dislocation would then interact less strongly with obstacles to its motion, particularly if the obstacle stress field is also screened by a hydrogen atmosphere. Following this line of reasoning, a stationary dislocation with a screening atmosphere should also interact less strongly with the applied stress. In order to initiate a significant amount of slip, that is, yielding, it would be necessary to apply a larger stress than without an atmosphere. This would correspond to the upper yield stress (Figure 3). Once the dislocations are forced to break free from their atmospheres and multiply, a smaller applied stress is required to move the dislocations, which are no longer shielded and can respond to the applied stress. This would correspond to the lower yield stress. The more concentrated the solute, the more dense the atmosphere and the larger is the screening. Thus, a larger applied stress is necessary to free the dislocations from their atmospheres, manifested in Figure 8 as an increase in yield stress with hydrogen concentration. This description of discontinuous yielding is functionally equivalent to the customary explanation that invokes pinning by an atmosphere. The failure to observe a strain aging effect using hydrogen can be explained by the insufficient number of hydrogen atoms to screen the greatly increased number of dislocations after initial yielding and multiplication.[36] For yielding at 77 K, the locking may be sufficiently strong and the unlocking stress so high that many other dislocation sources can progressively operate, resulting in smooth yielding (Figure 5).

C. *Work Hardening*

The dominant cause of work hardening is dislocation-dislocation interactions.[80] In solute-containing materials, the effect on the flow curve is a superposition of solute-dislocation interactions and dislocation-dislocation interactions.[81] Dislocation motion is not continuous but occurs in short bursts.[82] Dislocations sweep some area of the slip plane easily, only to be stopped at some obstacle where they wait for thermal activation. When the dislocation receives sufficient energy to be thermally activated over the barrier, it moves very rapidly until it meets the next obstacle. These obstacles could be other dislocations, precipitates, or solute clusters.[81]

Sirois *et al.*[61] have proposed that in hydrogen-charged specimens, every stationary obstacle to dislocation motion that has a dilatational stress field has its own atmosphere. They propose that when a dislocation is stopped at an obstacle, the hydrogen atoms in the atmospheres of the waiting dislocation and the obstacle reconfigure into positions of lowest energy; this is said to reduce the activation energy required to free the dislocation. Hence, the waiting time at obstacles is reduced and dislocations move with a higher average velocity. If the atmosphere moves with the dislocation, the dislocation is shielded from other stress centers, thus enhancing its mobility. The shielding effect of the hydrogen atmosphere depends on the high mobility of the hydrogen atoms and their ability to form atmospheres under the prevailing temperature and strain rate conditions.

The waiting time at obstacles is believed to be of the order of 1 s.[81] The time, t, required to form a hydrogen atmosphere around a stationary edge dislocation at 295 K can be estimated to be 10 ms. A similar calculation at 77 K shows that a hydrogen atmosphere will not form at a dislocation waiting at an obstacle, and hence shielding effects are not possible at this temperature. In our experiments, the work-hardening rates were found to decrease with increasing hydrogen concentrations at 295 K (Figure 4) but not at 77 K (Figure 6). This suggests that hydrogen diminishes the intensity of dislocation-dislocation interactions at room temperature, as expected from the calculations of Sirois *et al.*[61] At 77 K, however, hydrogen is unable to diffuse with or to dislocations and shield them at this low temperature.

Thus, a number of experimental observations can be explained provided the screening of the dislocation stress field is sufficiently strong. Unfortunately, this rationalization cannot easily explain the increased flow stresses as the amount of hydrogen is increased (Figures 3 and 5) nor the increase of work-hardening rate with hydrogen at 77 K (Figure 6). Both of these effects involve dislocations that are moving too fast to accumulate hydrogen atmospheres. We suggest that hydrogen exerts a global solute hardening for rapidly moving dislocations distinct from the local effect of atmosphere formation. It probably is due to interactions that are similar to carbon, nitrogen, or any other immobile solute species, *e.g.*, nickel or chromium in austenite. This has been attributed to energy dissipation as the dislocation passes an immobile strain center.[83] On the other hand, Nabarro has suggested that when a solute atom is able to change sites sufficiently rapidly, there could be an energy dissipation that is experienced as a drag on the dislocation.[83] Although this is not expected to be as large an effect at normal interstitial solute contents, it might be appreciable at the high concentrations of hydrogen used in this study. This effect would not be expected at 77 K, where the estimated jump rate is very low.

D. *Strain to Failure*

The strain to failure in our experiments was not critically dependent on hydrogen concentration (Figures 3 and 5), except at very high concentrations or intermediate temperatures where large reductions in measured elongation were observed. Our results can be compared with the expectations of the decohesion mechanism of hydrogen embrittlement[84] wherein hydrogen promotes cracking by weakening metal-metal bonds. The 310s specimens were clearly not weakened by the introduction of hydrogen. We are hence led to reject this hypothesis and look elsewhere for an explanation of hydrogen embrittlement. The dominant effect of hydrogen in 310s stainless steel is not to make cleavage easier but, apparently, to modify plastic behavior. It might be argued that this alloy is simply not degraded by hydrogen; after all, the values of elongation to failure are unaffected by up to 7 at. pct hydrogen. This may be explained as a thin foil effect, since the specimens were only a few grains thick. Thicker specimens have been shown to be embrittled by as low as 0.25 at. pct hydrogen.[85] The relatively small stress-enhanced concentration increase at the crack tip expected in that work would result in a lower concentration in the crack tip zone than in our thin specimens without a stress concentrator. However, slip-grain boundary interactions are less likely in these thin foil specimens, as are multiple slip interactions, since dislocations can pass out of the specimens relatively easily. Thus, we are led to conclude that hydrogen embrittlement is due to modification of slip behavior rather than a decrease in cohesion.

V. CONCLUSIONS

1. Except in the region of discontinuous yielding, the plastic regime of the true stress-strain curves of both hydrogen-free and hydrogenated 310s stainless steel specimens is fit very well by Ludwik's equation for specimens tested at various temperatures, strain rates, and hydrogen contents.
2. Hydrogen increases both the yield and flow stress of 310s stainless steel. This increase in strength is weaker than the strengthening effects of carbon and nitrogen in austenitic stainless steels.
3. Discontinuous yielding was observed in hydrogenated specimens tested at intermediate rates of strain for hydrogen contents greater than 5 at. pct at and near room temperature. Yield points were rarely observed at 77 K and, when present, were of very small magnitude.
4. The work-hardening rates were observed to decrease with hydrogen content for low strain values at 295 K, while at 77 K, the work-hardening rates increased with hydrogen content.
5. The strain to failure was not critically dependent on hydrogen concentration. Hydrogen did not cause embrittlement as measured by reduced elongation at the various temperatures studied, except at very high concentrations or intermediate test temperatures.

ACKNOWLEDGMENTS

The authors would like to thank the Allegheny-Ludlum Steel Company for supplying the stainless steel used in this work. Special thanks are also due to Professor H.K. Birnbaum for his helpful discussions. This work was supported by the Department of Energy under Contract No. DEFG02-91ER45439 through the Materials Research Laboratory, University of Illinois.

REFERENCES

1. H. Matsui, H. Kimura, and S. Moriya: *Mater. Sci. Eng.*, 1979, vol. 40, p. 207.

2. S. Moriya, H. Matsui, and H. Kimura: *Mater. Sci. Eng.*, 1979, vol. 40, p. 217.
3. H. Matsui, H. Kimura, and A. Kimura: *Mater. Sci. Eng.*, 1979, vol. 40, p. 227.
4. A. Kimura and H.K. Birnbaum: *Scripta Metall.*, 1987, vol. 21, p. 53.
5. I.M. Bernstein: *Scripta Metall.*, 1974, vol. 8, p. 343.
6. E. Lunarska: in *Hydrogen Degradation of Ferrous Alloys*, R.A. Oriani, J.P. Hirth, and M. Smialowski, eds., Noyes Publications, Park Ridge, NJ, 1985, p. 321.
7. E. Sirois and H.K. Birnbaum: *Acta Metall.*, 1992, vol. 40, p. 1377.
8. I.M. Robertson and H.K. Birnbaum: *Acta Metall.*, 1986, vol. 34, p. 353.
9. P. Rozenak, I.M. Robertson, and H.K. Birnbaum: *Acta Metall.*, 1990, vol. 38, p. 2031.
10. G. Bond, I.M. Robertson, and H.K. Birnbaum: *Acta Metall.*, 1988, vol. 36, p. 2193.
11. I.M. Robertson, T. Tabata, W. Wei, F. Heubaum, and H.K. Birnbaum: *Scripta Metall.*, 1984, vol. 18, p. 841.
12. T. Boniszewski and G.C. Smith: *Acta Metall.*, 1963, vol. 11, p. 165.
13. J.W. Watson, Y.Z. Shen, and M. Meshii: *Metall. Trans. A*, 1988, vol. 19A, pp. 2299-2304.
14. A.J. West and M.R. Louthan, Jr.: *Metall. Trans. A*, 1982, vol. 13A, pp. 2049-58.
15. G.R. Caskey, Jr.: *Scripta Metall.*, 1981, vol. 15, p. 1183.
16. J.H. Holbrook and A.J. West: in *Hydrogen Effects in Metals*, I.M. Bernstein and A.W. Thompson, eds., TMS-AIME, New York, NY, 1981, p. 655.
17. S. Asano and R. Otsuka: *Scripta Metall.*, 1976, vol. 10, p. 1015.
18. S. Asano and R. Otsuka: *Scripta Metall.*, 1978, vol. 12, p. 287.
19. M. Cornet and S. Talbot-Besnard: *Jpn. Inst. Metall. Suppl.*, 1980, vol. 21, p. 5454.
20. J. Burke, A. Jickels, P. Maulik, and L. Mehta: in *Effect of Hydrogen on the Behavior of Metals*, A.W. Thompson and I.M. Bernstein, eds., TMS-AIME, Warrendale, PA, 1976, p. 102.
21. D.G. Ulmer and C.J. Altstetter: *Acta Metall.*, 1991, vol. 28, p. 1237.
22. S.M. Myers, M.I. Baskes, H.K. Birnbaum, J.W. Corbett, G.G. DeLeo, S.K. Estreicher, E.E. Haller, P. Jena, N.M. Johnson, R. Kirchheim, S.J. Pearton, and M.J. Stavola: *Rev. Modern Phys.*, 1992, vol. 64, p. 559.
23. J.P. Hirth: in *Hydrogen Degradation of Ferrous Alloys*, R.A. Oriani, J.P. Hirth, and M. Smialowski, eds., Noyes Publications, Park Ridge, NJ, 1985, p. 131.
24. A.P. Bentley and G.C. Smith: *Scripta Metall.*, 1986, vol. 20, p. 729.
25. A.P. Bentley and G.C. Smith: *Mater. Sci. Technol.*, 1986, vol. 2, p. 1140.
26. M.B. Whiteman and A.R. Troiano: *Corrosion*, 1965, vol. 21, p. 53.
27. R.B. Benson, R.K. Dann, and L.W. Roberts: *Trans. TMS-AIME*, 1968, vol. 242, p. 2199.
28. M.L. Holzworth: *Corrosion*, 1969, vol. 25, p. 107.
29. M.R. Louthan, Jr., J.A. Donovan, and D.E. Rawl, Jr.: *Corrosion*, 1973, vol. 29, p. 108.
30. C.L. Briant: *Metall. Trans. A*, 1979, vol. 10A, pp. 181-89.
31. D. Eliezer: in *Hydrogen Effects on Material Behavior*, N.R. Moody and A.W. Thompson, eds., TMS, Warrendale, PA, 1990, p. 399.
32. T.-P. Perng and C.J. Altstetter: *Mater. Sci. Eng.*, 1990, vol. A129, p. 99.
33. J.A. Peterson, R. Gibala, and A.R. Troiano: *J. Iron Steel Inst.*, 1969, vol. 1, p. 86.
34. A.W. Thompson and I.M. Bernstein: *Adv. Corros. Sci. Technol.*, 1980, vol. 7, p. 53.
35. T.-P. Perng and C.J. Altstetter: *Acta Metall.*, 1986, vol. 34, p. 1771.
36. D.P. Abraham and C.J. Altstetter: *Metall. Mater. Trans. A*, 1995, vol. 26A, pp. 2859-2871.
37. J.A. Leistra and P.J. Sides: *J. Electrochem. Soc.*, 1987, vol. 134, p. 2442.
38. J. Dukovic and C.W. Tobias: *J. Electrochem. Soc.*, 1987, vol. 134, p. 331.
39. R.J. Coyle, A. Atrens, N.F. Fiore, J.J. Bellina, and M. Jolles: in *Environment Sensitive Fracture of Engineering Materials*, Z.A. Foroulis, ed., TMS-AIME, Warrendale, PA, 1979, p. 431.
40. D.G. Ulmer and C.J. Altstetter: *Acta Metall. Mater.*, 1993, vol. 41, p. 2235.
41. J. Crank: *The Mathematics of Diffusion*, Clarendon Press, Oxford, United Kingdom, 1956, p. 42.
42. H. Shih and H.W. Pickering: *J. Electrochem. Soc.*, 1987, vol. 134, p. 551.
43. G.E. Dieter: *Mechanical Metallurgy*, McGraw-Hill Publishing Co., New York, NY, 1976, p. 341.
44. T.H. Courtney: *Mechanical Behavior of Metals*, McGraw-Hill Publishing Company, New York, NY, 1990, pp. 80-85.
45. R.L. Fleischer: in *The Strengthening of Metals*, D. Peckner, ed., Reinhold Publishing Company, New York, NY, 1964, p. 114.
46. K. Oda, N. Kondo, and K. Shibata: *Iron Steel Inst. Jpn. Inst.*, 1990, vol. 30, p. 625.
47. R.P. Reed: *J. Met.*, 1989, Mar., p. 16.
48. H.M. Ledbetter and M.W. Austin: *Mater. Sci. Technol.*, 1987, vol. 3, p. 101.
49. E. Ligeon, R. Danielou, and J. Fontenille: *J. Appl. Phys.*, 1986, vol. 59, p. 108.
50. S.M. Myers, W.R. Wampler, and F. Besenbacher: *J. Appl. Phys.*, 1984, vol. 56, p. 1561.
51. S.T. Picraux: *Nucl. Instrum. Methods*, 1981, vol. 182–183, p. 413.
52. *Table of Periodic Properties of the Elements*, Catalog No. S-18806, E.H. Sargent and Co., Chicago, IL, 1964.
53. K. Tanaka, T. Inukai, K. Uchida, and M. Yamada: *J. Appl. Phys.*, 1983, vol. 54, p. 6890.
54. J.P. Hirth and J. Lothe: *Theory of Dislocations*, Wiley Publishing Co., New York, NY, 1982.
55. M.R. Louthan, Jr., G.R. Caskey, J.A. Donavan, and D.E. Rawl, Jr.: *Mater. Sci. Eng.*, 1972, vol. 10, p. 357.
56. M.R. Louthan, Jr.: in *Hydrogen in Metals*, I.M. Bernstein and A.W. Thompson, eds., ASM, Metals Park, OH, 1974, p. 53.
57. A.H. Cottrell: *Dislocations and Plastic Flow in Crystals*, Clarendon Press, Oxford, United Kingdom, 1953, p. 134.
58. A.H. Cottrell and B.A. Bilby: *Proc. Phys. Soc. London*, 1949, vol. A62, p. 49.
59. D.N. Beshers: *Acta Metall.*, 1958, vol. 6, p. 521.
60. D. Hull and D.J. Bacon: *Introduction to Dislocations*, Pergamon Press, Oxford, United Kingdom, 1984, p. 225.
61. E. Sirois, P. Sofronis, and H.K. Birnbaum: *Fundamental Aspects of Stress Corrosion Cracking*, Parkins Symp., S.M. Bruemmer, E.I. Meletis, R.H. Jones, W.W. Gerberich, F.P. Ford, and R.W. Staehle, eds., TMS, Warrendale, PA, 1992, p. 173.
62. F.R.N. Nabarro: *Theory of Crystal Dislocations*, Dover Publications, 1987, pp. 430-75.
63. N. Narita, C.J. Altstetter, and H.K. Birnbaum: *Metall. Trans. A*, 1982, vol. 13A, pp. 1355-65.
64. J.W. Steeds: *Proc. R. Soc.*, 1966, vol. A292, p. 343.
65. J.P. Hirth and B. Carnahan: *Acta Metall.*, 1978, vol. 26, p. 1795.
66. R. Kirchheim, X.Y. Huang, H.-D. Carstanjen, and J.J. Rush: in *Chemistry and Physics of Fracture*, R.M. Latanision and R.H. Jones, eds., 1987, p. 580.
67. R. Kirchheim: *Acta Metall.*, 1981, vol. 29, p. 845.
68. A. Kimura and H.K. Birnbaum: *Acta Metall.*, 1987, vol. 35, p. 1077.
69. P.A. Beaven and E.P. Butler: *Acta Metall.*, 1980, vol. 28, p. 1349.
70. A. Bourett and C. Colliex: *Ultramicroscopy*, 1982, vol. 9, p. 183.
71. W.H. Johnston and J.J. Gilman: *J. Appl. Phys.*, 1959, vol. 30, p. 129.
72. G.T. Hahn: *Acta Metall.*, 1962, vol. 10, p. 727.
73. H.C. Rogers: *Acta Metall.*, 1954, vol. 2, p. 167.
74. H.C. Rogers: *Acta Metall.*, 1957, vol. 5, p. 112.
75. H.C. Rogers: *Acta Metall.*, 1956, vol. 4, p. 114.
76. F. de Kazinczy: *Acta Metall.*, 1959, vol. 7, p. 706.
77. A. Lawley, W. Liebmann, and R. Maddin: *Acta Metall.*, 1961, vol. 9, p. 841.
78. C.J. Guntner and R.P. Reed: *Trans. ASM*, 1962, vol. 55, p. 399.
79. J. Eastman, F. Heubaum, T. Matsumoto, and H.K. Birnbaum: *Acta Metall.*, 1982, vol. 30, p. 1579.
80. D. Kuhlmann-Wilsdorf: *Mater. Sci. Eng.*, 1989, vol. A113, p. 1.
81. U.F. Kocks: *Metall. Trans. A*, 1985, vol. 16A, pp. 2109-29.
82. U.F. Kocks, A.S. Argon, and M.F. Ashby: *Progress in Materials Science*, Pergamon Press, Oxford, United Kingdom, 1975, vol. 19.
83. F.R.N. Nabarro: in *The Mechanics of Dislocations*, E.C. Aifantis and J.P. Hirth, eds., ASM, Metals Park, OH, 1985.
84. A.R. Troiano: *Trans. ASM*, 1960, vol. 52, p. 151.
85. J.H. Huang and C.J. Altstetter: *Metall. Trans. A*, 1991, vol. 22A, pp. 2605-18.